ADSORPTIVE REMOVAL OF Pb (II) USING EXFOLIATED GRAPHITE ADSORBENT: INFLUENCE OF EXPERIMENTAL CONDITIONS AND MAGNETIC $CoFe_2O_4$ DECORATION

NGUYEN THI THUONG[1,2], NGUYEN THI NGOC THU[3], BACH LONG GIANG[2], NGUYEN DUY TRINH[2], BUI THI PHUONG QUYNH[1]

[1]Faculty of Chemical Technology, Ho Chi Minh City University of Food Industry, Ho Chi Minh City, Vietnam
[2]NTT Hi-Technology Institute, Nguyen Tat Thanh University, Ho Chi Minh City, Vietnam.
[3]Faculty of Food, Chemical and Environmental Sciences, Nguyen Tat Thanh University, Ho Chi Minh City, Vietnam.

[*]Corresponding authors: quynhbtp@hufi.edu.vn; phuongquynh102008@gmail.com

(Received: 5th July 2018; Accepted: 17th April 2019; Published on-line: 1st June 2019)

https://doi.org/10.31436/iiumej.v20i1.965

ABSTRACT: The worm-like exfoliated graphite (EG) based adsorbents prepared from low-cost natural graphite flakes via facile synthesis processes have been found to be efficient adsorbents when it comes to removing Pb (II) from aqueous solution. EG was fabricated by chemical intercalation and microwave assisted exfoliation. Furthermore, the magnetic exfoliated graphite (MEG) was developed by incorporating $CoFe_2O_4$ particles into the EG layers using the citric acid based sol-gel technique. Adsorption behaviour of Pb (II) on the as-prepared adsorbents was investigated by taking several experimental conditions into consideration such as contact time, initial concentration, adsorbent dosage, and pH value. The results with initial neutral pH indicated that the adsorption isotherms for Pb (II) on the EG and MEG were well consistent with the Langmuir isotherm model revealing the maximum adsorption capacity of 106 mg/g and 68 mg/g for EG and MEG, respectively. The adsorption kinetics of Pb (II) was found to adhere to the pseudo-second-order kinetic model. The chemical interaction between π electrons on graphite sheets and Pb (II) ions was suggested to play an essential role in the adsorption mechanism. The introduction of magnetic $CoFe_2O_4$ to the EG was found to induce the shift of optimal pH value to a more basic condition. The characterization of the adsorbents was performed using relevant analysis techniques such as Scanning electron microscope (SEM), X–ray powder diffraction (XRD), vibrating-sample magnetometer (VSM), and Fourier-transform infrared (FTIR). The results of this work suggest a high possibility for the application of the as-prepared modified graphite to remove hazardous substances in practical wastewater treatment systems.

ABSTRAK: Penyerap Pengelupas Grafit (EG) yang berupa seperti cacing dihasilkan dari grafit semulajadi yang murah melalui proses sintesis serpihan, ia juga merupakan penyerap yang bagus dalam mengasingkan Pb (II) daripada larutan akues. EG direka dengan tindak balas interkalasi kimia dan pengelupasan melalui gelombang mikro. Tambahan, pengelupas grafit magnet (MEG) telah dihasilkan dengan memasukkan zarah $CoFe_2O_4$ ke dalam lapisan EG menggunakan teknik sol-gel yang berasaskan asid sitrik. Tindak balas penyerapan Pb (II) pada penyerap yang disiapkan ini, dikaji dengan mengambil kira beberapa keadaan eksperimen

seperti waktu disentuh, konsentrasi awal, dos penyerap dan nilai pH. Hasil keputusan pH neutral awal menunjukkan bahawa isoterm penyerapan bagi Pb (II) pada EG dan MEG adalah konsisten dengan model isoterm Langmuir. Ini menunjukkan kapasiti penyerapan maksimum 106 mg/g dan 68 mg/g bagi EG dan MEG, masing-masing. Penyerapan kinetik Pb (II) didapati mematuhi model kinetik pesudo-order-kedua. Interaksi kimia antara elektron π pada helaian grafit dan ion Pb (II) memainkan peranan penting dalam mekanisme penyerapan. Pengenalan magnet $CoFe_2O_4$ kepada EG didapati telah mengubah nilai pH optimum kepada keadaan asal. Pengelasan penyerapan dilakukan menggunakan teknik analisis yang relevan seperti Mikroskop Elektron Pengimbasan (SEM), Difraksi Serbuk sinar-X (XRD), Magnetometer Sampel-Getaran (VSM) dan Inframerah Perubahan-Fourier (FTIR). Hasil kerja ini mencadangkan kemungkinan besar bagi penggunaan grafit ubah suai yang disediakan bagi membuang bahan berbahaya dalam sistem rawatan air sisa praktikal.

KEYWORDS: *adsorption; heavy metal; exfoliated graphite; Pb (II) ions; wastewater treatment*

1. INTRODUCTION

In the past decades, environmental contamination due to the presence of heavy metals in wastewater from industrial processes and products has increasingly grown. Heavy metal contamination adversely affects human health and organisms due to the high toxicity of metal ions even at low metal concentration. Among many kinds of heavy metals, lead (Pb) poisoning has caused a major public health risk as it can lead to symptoms like delirium, convulsions, persistent vomiting, coma, and also cause serious damage to hematopoietic, central nervous, and reproductive systems [1]. Thus, the efficient decontamination of water containing Pb^{2+} has been considered as one of the most important tasks for environmental scientists. There are various techniques for this, including membrane filtration, solvent extraction, chemical precipitation, and adsorption. Among the aforementioned techniques, the adsorption method is still more favoured since it can offer many important benefits such as high removal efficiency, simple operation, wide adaptability, recyclability, and economic feasibility.

Among a cascade of adsorbents developed for decontamination of heavy metals, a number of products from graphite have been demonstrated to be very efficient [2-7]. The adsorption behaviour of heavy metal ion appeared to depend strongly on the textural, physical, and chemical properties of graphite related adsorbents that are essentially determined by the synthesis approach. In attempts to obtain high adsorption capacity, several preparation protocols and precursors have been employed. For instance, graphene layers fabricated from graphite rods by complete exfoliation to graphene layers containing 30 wt.% PF^{6-} showed high adsorption capacity for Pb^{2+} (406.6 mg/g) and Cd^{2+} (73.42 mg/g) [2]. Additionally, the lead ion uptake of graphene nanosheets was found to be significantly improved under vacuum heat treatment [3]. Reportedly, the introduction of Fe_3O_4 particles onto graphene platforms could support high removal efficiencies and fast adsorption rates for Cu^{2+}, Cd^{2+} and Pb^{2+} [5]. In another work [4], the graphene surface modified by iron nanoparticles exhibited the maximum adsorption capacity of 4.86, 3.26, and 6.00 mg/g for Cr(VI), As(V), and Pb (II) respectively at an initial metal ion concentration of 5.0 ppm. More recently, high removal efficiency of Pb (II) and Cd (II) ions were achieved using the composite of a significant amount of spinel magnetic particles and graphene sheets [6]. The adsorption of heavy metals on graphene-related materials was suggested to occur via chemical interaction of functional groups on the

adsorbent surface. Despite very high adsorption capacity and fast adsorption kinetics, the practical application of graphene/graphene oxide structured materials in the removal of hazardous substances still faces several difficulties including the cost and the complication of their fabrication process.

Owing to its layered structure, graphite can allow easy addition of various atoms and molecules into these layers to form graphite intercalated compounds (GICs). Exfoliated graphite (EG) is a modified graphite material that has a certain expansion degree of distance between the carbon layers afforded via thermal exfoliation of the GICs. The exfoliation process can be obtained by either using microwave irradiation or thermal shock [8-15]. The EG exhibits fascinating properties such as low density, large surface area, and a worm-like porous structure and thus has found a number of applications such as electromagnetic interference shielding, electrochemical electrodes, vibration damping, and, recently, purification of oil-polluted water [16,17]. However, the utilization of EG can cause some problems due to difficulty in gathering the low-density materials after adsorption. In order to restrict this shortcoming, the magnetic component was added to the EG adsorbent to allow easy recovery of the used adsorbents from wastewater under a magnetic field [18-21].

Herein, we developed efficient adsorbents from the low-cost, abundantly available natural graphite flakes for remediation of lead-contaminated water. The exfoliation of graphite flakes was assisted by microwave irradiation, which is advantageous over conventional heating in terms of efficient, uniform heat distribution, and short-time treatment. Furthermore, a sufficient amount of magnetic $CoFe_2O_4$ species was incorporated into the exfoliated graphite layers via the simple citric acid based sol-gel process to afford the feasible collection of used materials from solution under an applied magnetic field. The presence of a small amount of $CoFe_2O_4$ particles between the graphite sheets can not only provide EG with susceptibility to magnetic field but can also help stabilize the structure of expanded graphite layers. The adsorption of Pb (II) was studied taking into account the effects of various experimental factors including adsorbent dosage, initial Pb^{2+} concentration, contact time, and pH value. The adsorption isotherms and adsorption kinetics were interpreted using the relevant adsorption models. Properties of the adsorbents were analyzed using SEM, XRD, VSM and FTIR techniques.

2. EXPERIMENTAL PROCEDURE

2.1 Chemicals and Materials

Natural flake graphite with granule size > 1.25 mm and carbon content ≥ 85% was collected in Yen Bai province, Vietnam. Chemicals including H_2SO_4 (98%) and H_2O_2 (30%), $Fe(NO_3)_3.9H_2O$, $Co(NO_3)_2.6H_2O$, $NH_4.OH$, $Pb(NO_3)_2$ were supplied by Guang Chemical Company, China.

2.2 Preparation of the Exfoliated Graphite (EG) and the Magnetic Decorated Exfoliated Graphite (MEG)

The EG was synthesized by intercalation method using H_2O_2 as an oxidizing agent and H_2SO_4 as an intercalating agent as follows. Natural graphite flakes were added into the mixture of H_2SO_4 and H_2O_2 (20:1.6 v/v). After 50 minutes, the intercalated mixture was continually washed with water until the pH value reached 5-6. Then, the resulting black powder was collected by vacuum filtering and dried in an oven. The EG was obtained by exfoliation in a microwave oven at the power of 750 W for 10 s. In the next step, the magnetic $CoFe_2O_4$ nanoparticles were then introduced to EG surface by sol-gel method as

the following procedure. A mixture of $Fe(NO_3)_3.9H_2O$, $Co(NO_3)_2.6H_2O$ (with molar ratio of Fe^{3+}/Co^{2+}= 1:2) were homogeneously dissolved in 0.02 M citric acid solution (with molar ratio of acid/Fe^{3+} = 4:1). In order to keep the sols stable, the solution had the pH regulated to about 7-8. Following this, EG was added and the solution was stirred for up to 30 minutes or until the floating EG disappeared on the surface of the solution. The obtained composites were further baked in a furnace at 600 ºC for 1 hour.

2.3 Adsorption Experiments

In the batch adsorption experiments, Erlenmeyer flasks containing 50 ml of aqueous solution of Pb (II) ions and a predetermined amount of absorbent were shaken at 200 rpm for 2 h. The residual concentrations of heavy metals were confirmed by AAS analysis. The removal efficiency and the adsorption capacity (q_e) were calculated as follows:

$$\text{Percentage removal} = \frac{C_o - C_e}{C_o}.100 \quad (1)$$

Where C_o and C_f are the initial and equilibrium Pb (II) concentrations (ppm), respectively.

$$q_e = \frac{C_o - C_e}{W}.V = \frac{C_o - C_e}{d_{adsorbent}} \quad (2)$$

where V (ml) is the volume of the Pb (II) solution, W (g) is the weight of the adsorbent, $d_{adsorbent}$ (g/l) is the dosage of the adsorbent.

Investigated input factors included shaking time, initial Pb (II) concentration, adsorbent dosage, and pH of solution. The processes are as follows. First, the effect of contact time on lead (II) adsorption was conducted by shaking the mixture of 3 g/l of adsorbent and 100 ppm of Pb (II) concentration in different time intervals (10-360 min) in a neutral medium. Second, the effect of the initial lead concentration was studied by adding 3 g/l of adsorbent to Pb (II) solution of various concentrations (10-600 ppm) in a neutral medium for 120 min. Third, for adsorbent dosage, we investigated its effect by varying EG dosage from 1 g/l to 6 g/l, where the initial concentration of Pb (II) ions and contact time were 100 ppm and 120 min, respectively in a neutral medium. Lastly, the investigation of the effect of initial pH was conducted by varying pH value from 2 to 12 in initial Pb (II) solution of 100 ppm and adsorbent dosage of 3 g/l for 120 min.

2.4 Characterization Methods

The X–ray powder diffraction (XRD) of AC was recorded on a D8 Advance Bruker powder diffractometer with a Cu–Kα excitation source at a scan velocity of 2º (2θ) min^{-1}. The angle range (2θ) was investigated between 0º and 50º. A scanning electron microscope (SEM) technique was employed on the S4800, Japan instrument to investigate the morphology of adsorbent surface. Fourier transform infrared (FT-IR) analysis of samples was determined using a Bruker ALPHA FT-IR spectrophotometer with KBr as a matrix in the range of 4000−400 cm^{-1}. To determine specific surface area and porous structure, the nitrogen adsorption/desorption measurement of adsorbent was performed on Nova Station B. A GMW 3474-140 magnetometer equipped with a superconducting magnet capable of producing fields up to 16 Koe was used to measure static magnetic moment. To detect the amount of Pb (II) ions remaining in solution, atomic absorption spectroscopy (AAS) measurement was conducted with AA 6800 Shimadzu equipment.

3. RESULTS AND DISCUSSION

3.1 Adsorptive Removal of Pb (II) using the Exfoliated Graphite (EG)

3.1.1 Characterization of the Exfoliated Graphite

Morphology of the graphite flake and the EG were characterized by SEM as presented in Fig. 1. It can be seen that structure of the graphite consists of rigidly stacking multilayers (Fig. 1a). After the intercalation followed by microwave exfoliation, the worm-like particles and layered aggregative structure with interconnected open pores are shown in Fig. 1b. A closer view in Fig. 1c reveals a multi-porous structure. Figure 2 reveals N_2 adsorption/desorption curves of NG and EG. It can be seen that the type IV isotherm was determined for EG which indicates the existence of a large number of mesopores and very little micropores in graphite-based adsorbents. The obtained results showed that the specific surface area for the EG is 30.0 m^2/g while such parameter of raw graphite is 6.5 m^2/g, implying the formation of highly porous structure after exfoliation process.

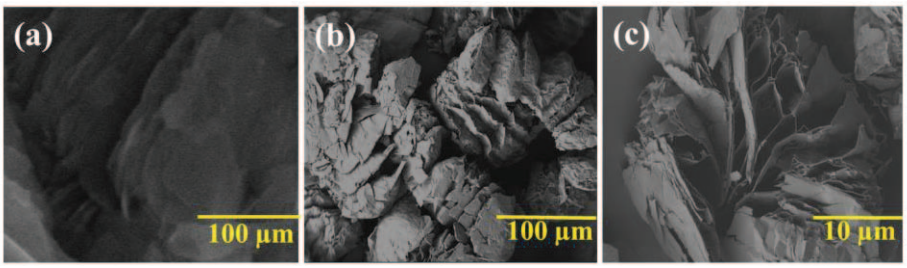

Fig. 1: SEM images of the graphite (a) and EG (b, c).

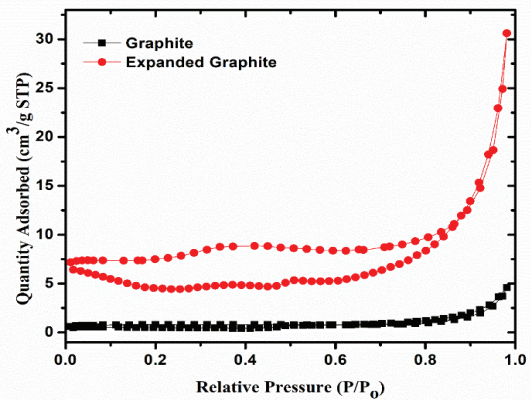

Fig. 2: The N_2 adsorption/desorption isotherm curves of graphite and expanded graphite.

3.1.2 Effects of Experimental Conditions on Adsorption Behavior of Pb^{2+} on EG

The influence of the contact time on the percentage removal of Pb (II) using EG adsorbent was displayed in Fig. 3a. Visually, prolonged contact leads to increased lead ion adsorption and equilibrium was attained after shaking for 120 min. Initially, the removal of Pb (II) occurred rapidly, reaching approximately 75% within the first 50 min. The adsorption then rises gradually before reaching the saturated level at 81.8 % at 120 min. The high initial adsorption rate of Pb^{2+} on EG can be attributed to easy diffusion of lead ions to its large external surface area and possibly into the wrapping adsorption space between stacking layers and large pores in each particle [6]. After 50 min, the significant occupation of Pb^{2+} ions inside the pores and also on the external surface may become a

barrier hindering the contact between the active sites and other Pb^{2+} ions thus resulting in a slower adsorption rate. Based on this result, further adsorption experiments were all conducted in 2 hours.

Regarding initial concentration, the graph suggested that this factor induced a downward trend to the adsorption of Pb (II) at a fixed EG dosage (Fig. 3b). The efficiency dropped from 81.6% to 26% as the concentration increased from 100 ppm to 600 ppm. At low initial concentration, increased availability of adsorption sites could easily bind the Pb (II) ions [3]. As the concentration of Pb^{2+} ion in the solution was higher than the adsorption capacity of the EG, the removal efficiency started to drop. By contrast, the increment of adsorbent dose from 1 g to 6 g/l increased the percentage removal of Pb (II) from 45.2% to 89% (Fig. 3c). The efficiency of lead uptake steadily rose with as the adsorbent dose increased from 1 g/l to 3 g/l but further addition of EG up to 6 g/l just afforded a slight enhancement in percentage removal. It can be explained that increasing the adsorbent dose provided a greater amount of active sites to capture metal ions thus allowing higher treatment efficiency.

The relationship between adsorption of Pb^{2+} and the pH value of the solution is presented in Fig. 3d. It can be observed that variation of pH value between 2 and 8 did not significantly alter the Pb^{2+} uptake on EG while the adsorption was much more favoured in strongly basic solution, as evidenced by a steady increase (from 74% to 97%) in removal efficiency in relation to increased pH value of 10 and 12. In more basic condition, the decreased competition of H^+ led to an increase in the adsorption of lead ions. Justification for that could be the protonated surface functional groups and severe competition with the adsorption of lead ions caused by excess H^+ at low pH values [22]. At the pH of 12, the removal percentage achieved its highest level of almost 97%, possibly owing to the combined effect of adsorption and precipitation [3].

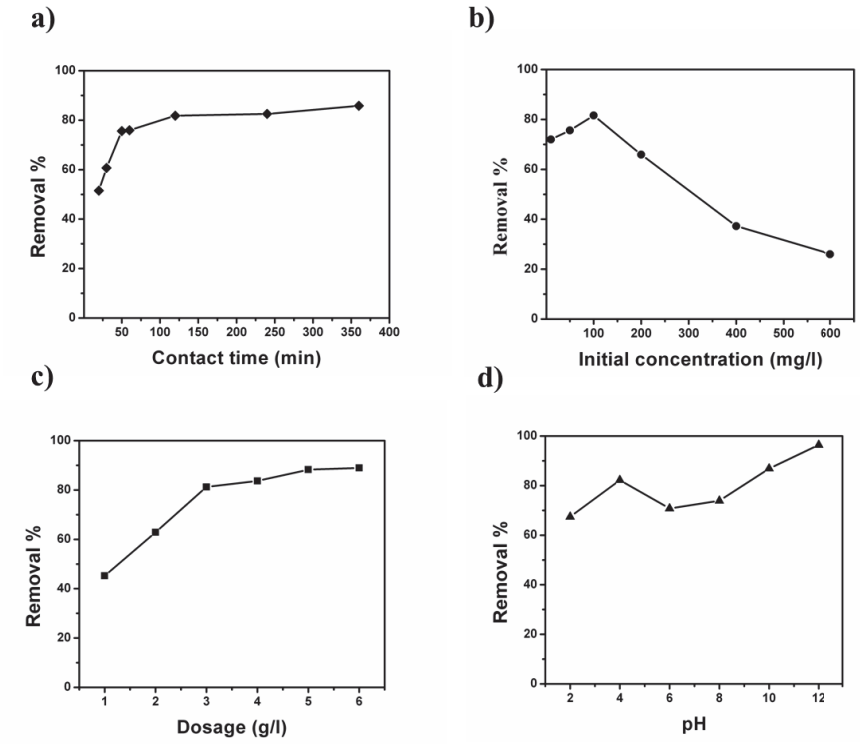

Fig. 3: The effect of adsorbent dosage (a), the initial concentration (b), the contact time (c) and the pH (d) on the removal efficiency of Pb (II) using EG.

3.1.3 Adsorption Kinetics and Adsorption Isotherms

In order to analyse the adsorption kinetics, we fit the experimental data with the linear form of the pseudo-first-order and pseudo-second-order kinetic models described respectively as follows:

$$\log(q_e - q_t) = \log q_e - \left(\frac{k_1}{2.303}\right) t \quad (3)$$

$$\frac{t}{q_t} = \frac{1}{k_2 q_e^2} + \left(\frac{1}{q_e}\right) t \quad (4)$$

where q_e (mg/g) is the amount of pollutant adsorbed at equilibrium, q_t (mg/g) is the amount of pollutant adsorbed at time t, k_1 (min^{-1}) is the pseudo-first-order rate constant, and k_2 (g/mg.min) is the pseudo-second-order rate constant [23]. Estimated parameters of the two models are summarized in Table 1. The high correlation coefficient R^2 (0.9984) shows good consistency between he pseudo-second order kinetic model and the experimental data. In contrast, the fitting to the pseudo-first-order kinetic model was more deviated as demonstrated by a lower correlation coefficient (R^2 = 0.7255).

Table 1: Isotherm and kinetics parameters for the adsorption of Pb (II) on EG

Pseudo-first-order		**Pseudo-second-order**		**Langmuir isotherm**		**Freundlich isotherm**	
$q_{e(mg/g)}$	5.3150	$q_{e(mg/g)}$	27.7008	$q_{e(mg/g)}$	106.3830	K_F	1.5866
k_1 (min^{-1})	0.0076	k_1 (min^{-1})	0.0058	K_L (l/mg)	0.0109	1/n	0.572
R^2	0.7255	R^2	0.9984	R^2	0.9768	R^2	0.8158
				R_L	0.1867		

The way in which the adsorbates interact with EG adsorbent is crucial and could be described via adsorption isotherms. Such isotherms give some insights into the adsorption process and provide important parameters to disclose the adsorption mechanism. Reportedly, Langmuir and Freundlich isotherms could accurately characterize the adsorption behaviour of heavy metals on various substrates. The Langmuir isotherm model is based on the assumption that the adsorption occurs at specific homogeneous sites within the adsorbent and there is no significant interaction among adsorbed species [24]. The following equation presented the Langmuir isotherm [23]:

$$\frac{1}{q_e} = \frac{1}{q_m} + \frac{1}{K_L q_m C_e} \quad (5)$$

where q_e (mg/g) is the amount of adsorbates adsorbed at equilibrium, q_m (mg/g) is the maximum monolayer adsorption capacity of the adsorbent, C_e (mg/l) is the concentration of the adsorbate under equilibrium condition and K_L (l/mg) is the Langmuir constant. From Langmuir's model, the separation factor R_L is calculated as follows:

$$R_L = \frac{1}{1+K_L C_o} \quad (6)$$

where C_0 (mg/l) is the highest metal concentration in solution and K_L (l/mg) is the Langmuir constant. Adsorption is considered (i) unfavourable if $R_L > 1$, (ii) linear if $R_L = 1$, (iii) favourable if $0 < R_L < 1$ and (iv) irreversible if $R_L = 0$. From Table 1, it could be concluded that the adsorption of Pb (II) onto the surface of EG was favourable since the calculated R_L value fell within 0 and 1. Values of the constants can be deduced from the Figure 4c, which plotted linear relationship of ($1/q_e$) versus ($1/C_e$).

Inherent within the Freundlich isotherm model, it is assumed that the stronger binding sites are occupied first and the affinity for binding is inversely proportional with number of occupied sites due to the adsorption of adsorbates onto heterogeneous surfaces. The Freundlich isotherm is defined as the following equation:

$$\ln q_e = \ln K_F + \frac{1}{n}\ln C_e \quad (7)$$

where K_F [(mg/g).(l/mg)^n] is Freundlich constant and 1/n is the adsorption intensity. The value of 1/n indicates that adsorption is favourable (n < 1, monolayer adsorption) and a value more than 1 implies cooperative adsorption.

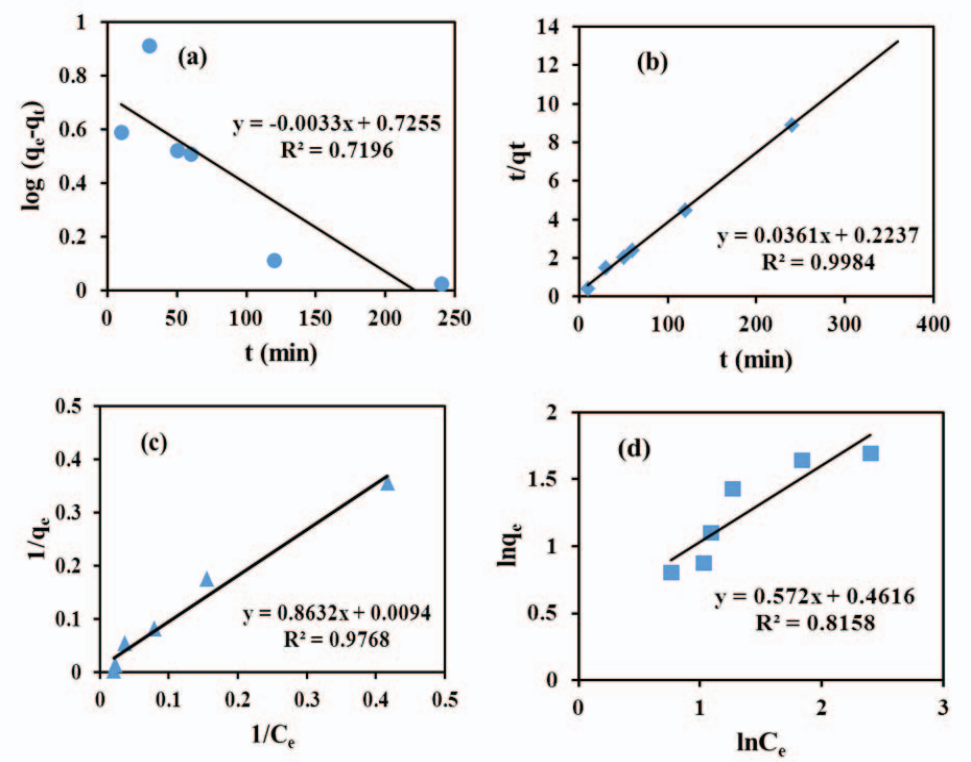

Fig. 4: Adsorption kinetics and isotherms for Pb (II) ions: Pseudo-first-order (a) and pseudo-second-order (b) kinetic plot, Langmuir (c) and Freundlich (d) adsorption isotherm of the EG.

Langmuir isotherm and Freundlich isotherm showed correlation coefficients (R^2) of 0.9768 and 0.8158 respectively for Pb (II) ions on graphite layers. These results suggested the close fit of experimental data of adsorption for Pb (II) ion with the Langmuir isotherm model (R^2=0.98) indicating the formation of Pb^{2+} monolayers over EG surface. The maximum adsorption capacity of Pb (II) ions onto EG was calculated to be 106 mg/g. In addition to this, the adsorption of EG for Pb (II) ions was favourable since the R_L value was found to be between 0 and 1.

3.1.4 FTIR Analysis

Recorded FTIR spectra of before and after Pb (II) adsorption representing the mechanism of adsorption of Pb (II) ions on the EG is presented in Figure 5. The spectrum of EG reveals the presence of characteristic peaks as follows: 3445 cm^{-1} (stretching vibration of OH), 2967 cm^{-1} (stretching vibration of C-H in CH, CH_2 and CH_3), 1635 cm^{-1} (stretching vibration of C=O), 1385 cm^{-1} (blending and scissor vibration of CH_3 and CH_2), 1048 cm^{-1} (stretching vibration of C-O), 790 cm^{-1} (deformation vibration of the CH_2 bond)

[25,26]. During adsorption process, there were some interactions between the EG and Pb (II) ions in the aqueous phase, consequently resulting in shifts of the characteristic peaks. As observed in Fig. 5, the adsorption peak at 3445 cm^{-1} before shifting towards 3450 cm^{-1} is possibly caused by the bonding of OH^- with Pb (II) ions [27]. Moreover, the shifts of 2967, 1635, 1385, 1048 and 790 cm^{-1} to 2925, 1626, 1390, 1049 and 797 cm^{-1}, respectively, can be easily recognized. These shifts might be ascribed to electrostatic interaction between the π electrons of graphite layers and Pb^{2+} ions [28]. Note that both the external surface and internal surface of pores in EG can take part in the adsorption of Pb^{2+} efficiently. Moreover, it is worthy to note that the curled structure of EG could possibly behave like a heavy metal trap and wrapped up Pb (II) ions inside the pores as similar with the function of nanotube-structured adsorbent.

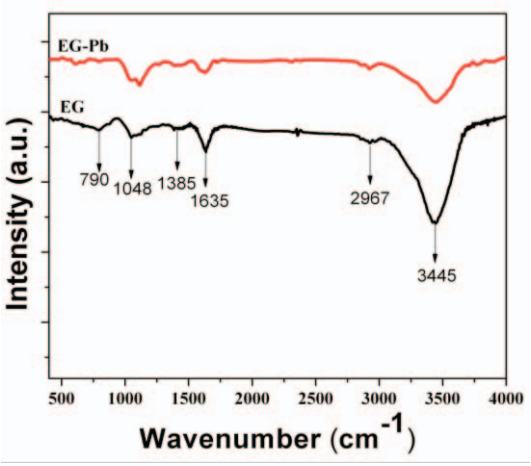

Fig. 5: FTIR spectra of EG and Pb (II) adsorbed EG.

3.2 Adsorptive Removal of Pb (II) Using the Magnetic Decorated MEG

3.2.1 Characterization of MEG

To enable collection of EG using a magnetic field, $CoFe_2O_4$ particles were introduced to the exfoliate d graphite layers by the citric acid based sol-gel process. In attempts to achieve sufficient magnetic susceptiblity with minimized metal oxide loading, the influence of different EG/$CoFe_2O_4$ ratios was considered. Figure 6a illustrated the separation of MEG samples under external magnetic field. The nearly complete separation was obtained with the EG:$CoFe_2O_4$ ratio of 1:1 and 3:1 while the ratio of 5:1 appeared insuffficient. This phenomenon agreed well with results analyzed using VSM measurement at room temperature. Figure 6b showed that the magnetization hysteresis loops of MEG were the S-like curves; the saturation magnetization values (Ms) increased strongly from 5 emu/g to 32 emu/g when reducing the EG/$CoFe_2O_4$ weight ratio from 5:1 to 3:1 but further decrease of this ratio to 1:1 just slightly enhanced the Ms to 42 emu/g. Since the EG/$CoFe_2O_4$ ratio of 3:1 with Ms of 32 emu/g was able to allow feasible magnetic separation, this ratio was selected for further investigation.

As observed in Fig. 6c, besides the peaks characteristic of EG structure, the additional appearance of a small peak at $2\theta = 35.5$ can be ascribed to the (311) plane of the $CoFe_2O_4$ [29,30]. Furthermore, the disappearance of the peak at 44.4° in the spectrum of modified EG implied that graphite sheets were further expanded during the heat treatment at 600 °C. The successful incorporation of $CoFe_2O_4$ particles into EG layers were also confirmed by the SEM analysis. Figure 6d shows the morphology of MEG as investigated by SEM analysis. The MEG surface was found to consist of various wrinkled and folded domains

evenly decorated with $CoFe_2O_4$ particles in the nanosize range (about 50-80 nm) without large aggregations (inset of Fig. 6d). These analysis results prove the successful incorporation of magnetic property to the EG via addition of nanosized $CoFe_2O_4$ particles.

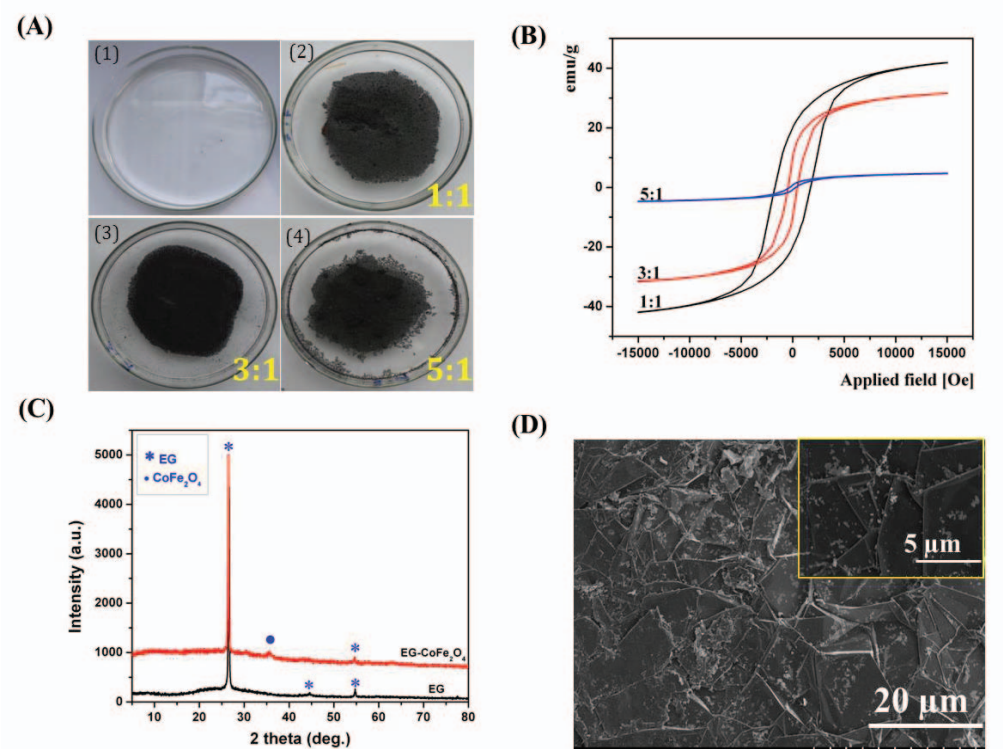

Fig. 6: Properties of magnetic $CoFe_2O_4$-EG samples; (A), inset (1): solution without MEG, (2) EG:CoF_2O_4 = 1:1, (3) EG:CoF_2O_4 = 3:1 and (4) EG:CoF_2O_4 = 5:1; (B) the magnetization hysteresis loops of MEG: $CoFe_2O_4$; (C) XRD and (D) SEM of MEG (EG:CoF_2O_4 = 3:1).

3.2.2 Effect of Experimental Conditions on Adsorption Behaviour of Pb^{2+} on the MEG

Impacts of various experimental factors on the percentage removal of Pb^{2+} using MEG adsorbent were shown in Fig. 7. In general, the change tendency is quite similar with EG but MEG exhibited lower Pb^{2+} uptake than EG in neutral solution. For instance, at the fixed concentration of 100 ppm, dosage of 3 g/l, in a neutral environment, the time to obtain equilibrium condition was 60 min, which was much shorter than in the case of EG (Fig. 7a). This is partly ascribed to the adsorbate-adsorbate steric effects [31]. When the expanded graphite was covered by $CoFe_2O_4$ species, a number of functional groups responsible for metal binding, on either external surface or internal surface of pore channels, may be blocked by $CoFe_2O_4$ species thus resulting in decrease in adsorption performance. Although the $CoFe_2O_4$ incorporation was found to reduce the adsorption capacity of EG, it still possessed a significant adsorption capacity for practical application. At the MEG dosage of 3 g/l, the removal efficiency dropped from about 70% to 22 % when increasing the initial Pb^{2+} concentration from 10 ppm to 600 ppm (Fig. 7b). Raising the MEG dosage from 1g/l to 6 g/l also induces a 60 point rise in the percentage removal from 22 % to about 82% (Fig. 7c). It can be deduced that the deposition of $CoFe_2O_4$ nanoparticles inside the pores may block the diffusion of metal ions to internal surface of carbon layers, limiting adsorption capacity and deferring equilibrium of EG (as compared to unmodified EG).

The pH value appeared to have more significant impact on the adsorption process on MEG than on EG. As can be seen from Fig. 7d, an upsurge in percentage removal (from 22% to nearly 100%) was observed with increasing pH from 2 to 8. Accordingly, the optimal pH condition for adsorption on MEG can be defined in the range of 8-10. It means that the optimal pH value was shifted to less basic condition after incorporation of $CoFe_2O_4$. Compared to EG, adsorption of Pb^{2+} on MEG in the pH range of 8-10 was higher (80% vs 96%), which likely indicate the presence of synergistic effect afforded by $CoFe_2O_4$, carbon layers and hydroxide species present in the solution.

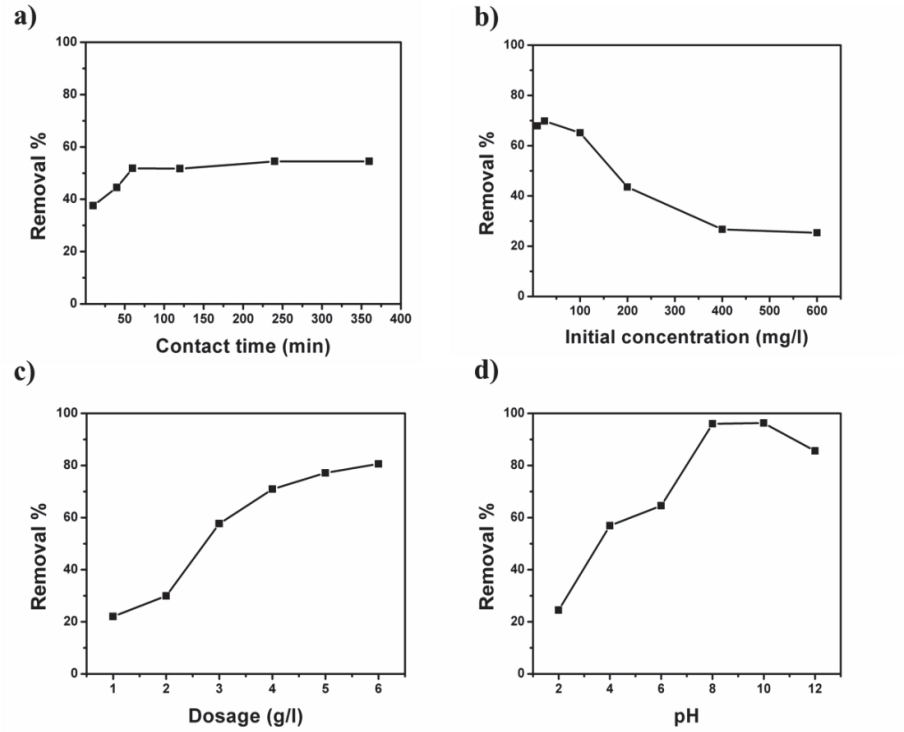

Fig. 7: The effects of contact time (a), initial concentration (b), adsorbent dosage (c) and pH (d) on the removal efficiency of Pb (II) using the MEG.

3.2.3 Adsorption Kinetics and Adsorption Isotherms

The studies of adsorption kinetics and isotherms for MEG were performed in the similar experimental conditions with EG. The derived model parameters are summarized in Table 2. The plots for pseudo-first order and pseudo-second order models are illustrated in Fig. 8a and 8b. In a similar manner with EG, the pseudo-second-order kinetic model was found to fit well with adsorption data for the $CoFe_2O_4$ decorated EG as evidenced by a high correlation coefficient (R^2 = 0.9997). The rate constant k_1 for MEG was found higher than that for EG (0.0071 vs 0.0058).

Table 1: Isotherm and kinetics parameters for the adsorption of Pb (II) on EG

Pseudo-first-order		**Pseudo-second-order**		**Langmuir isotherm**		**Freundlich isotherm**	
$q_{e(mg/g)}$	6.1404	$q_{e(mg/g)}$	18.5529	$q_{m(mg/g)}$	68.0272	K_F	0.6208
k_1 (min^{-1})	0.0021	k_1 (min^{-1})	0.0071	K_L (L/mg)	0.0109	1/n	1.5212
R^2	0.8665	R^2	0.9997	R^2	0.9936	R^2	0.9364
				R_L	0.1323		

The plots of Langmuir and Freundlich isotherms are presented in Fig. 8c and 8d. Again, the Langmuir model still best described the adsorption behaviour of Pb^{2+} on MEG (R^2 = 0.9936). The correlation coefficient from Freundlich model was lower at 0.9364. The maximum adsorption capacity as calculated from Langmuir equation was 68 mg/g. The R_L value of 0.1323 indicates favourable adsorption as found between 0 and 1.

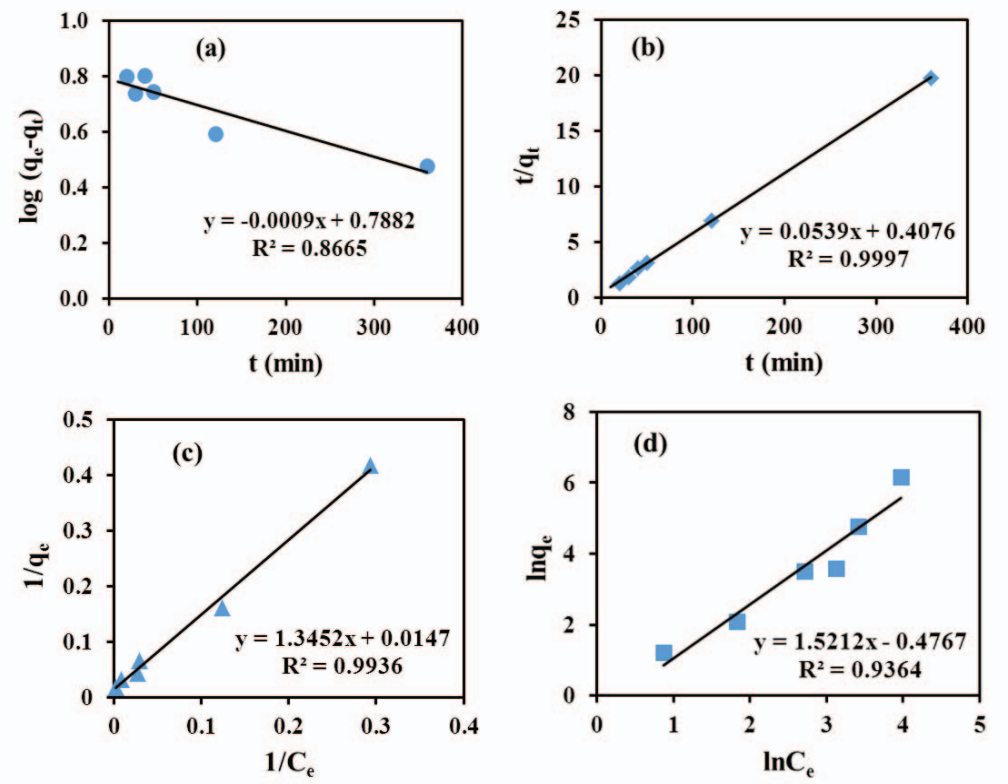

Fig. 8: Adsorption kinetics and isotherm for Pb (II) ion: (a) Pseudo-first-order (a) and pseudo-second-order kinetic plots (b), Langmuir (c) and Freundlich isotherms (d) of the MEG.

4. CONCLUSION

Efficient exfoliated graphite-based adsorbents for Pb^{2+} elimination from aqueous solution were developed from the low-cost, abundantly available natural graphite flakes via facile preparation procedures. The magnetic EG was also fabricated by incorporation of $CoFe_2O_4$ particles into the exfoliated graphite layers. Adsorption capacity of EG and MEG for Pb (II) ions increased with higher adsorbent dosage, contact time and pH and decreased as initial concentration of Pb (II) increased. The pseudo-second order kinetic model and Langmuir model are two models that well described adsorption behaviour of Pb (II) ions onto both as-prepared EG and $CoFe_2O_4$ decorated EG. The Langmuir equation suggested that the maximum adsorption capacity of EG and MEG for Pb^{2+} ions were 106 and 68 mg/g, respectively. The presence of $CoFe_2O_4$ particles in the carbon layers shortened the contact time to equilibrium, reduced the elimination efficiency in neutral solution but increased that in more basic solution (pH = 8-10). It is suggested that the binding Pb (II) ions to EG surface was afforded due to its curled structure and chemical interaction between π electrons of carbon layers and positively charged metal ions. According to the obtained results, the as-prepared EG and MEG with advantages of low-cost and abundantly available graphite precursor, non-complicated fabrication process and

significant adsorption capacity hold reasonable practicality for treating water for heavy metal contamination.

ACKNOWLEDGEMENT

This work was supported by the KIST Institutional Program (Project No. 2Z04820-16-090).

REFERENCES

[1] Flora G, Gupta D, Tiwari A. (2012). Toxicity of lead: A review with recent updates. Interdisciplinary Toxicology, 5:47-58.
[2] Deng X, Lu L, Li H, Luo F. (2010). The adsorption properties of Pb(II) and Cd(II) on functionalized graphene prepared by electrolysis method. Journal of hazardous materials, 183:923-930.
[3] Huang ZH, Zheng X, Lv W, Wang M, Yang QH, Kang F. (2011). Adsorption of lead(II) ions from aqueous solution on low-temperature exfoliated graphene nanosheets. Langmuir : the ACS journal of surfaces and colloids, 27:7558-7562.
[4] Gollavelli G, Chang C-C, Ling Y-C. (2013). Facile Synthesis of Smart Magnetic Graphene for Safe Drinking Water: Heavy Metal Removal and Disinfection Control. ACS Sustainable Chemistry & Engineering, 1:462-472.
[5] Zhang W, Shi X, Zhang Y, Gu W, Li B, Xian Y. (2013). Synthesis of water-soluble magnetic graphene nanocomposites for recyclable removal of heavy metal ions. Journal of Materials Chemistry A, 1:1745-1753.
[6] Santhosh C, Kollu P, Felix S, Velmurugan V, Jeong SK, Grace AN. (2015). $CoFe_2O_4$ and $NiFe_2O_4$@graphene adsorbents for heavy metal ions - kinetic and thermodynamic analysis. RSC Advances, 5:28965-28972.
[7] Pourbeyram S. (2016). Effective Removal of Heavy Metals from Aqueous Solutions by Graphene Oxide–Zirconium Phosphate (GO–Zr-P) Nanocomposite. Industrial & Engineering Chemistry Research, 55:5608-5617.
[8] Kim J, Kim H, Kim B, Jeon K-J, Yoon S-H. (2014). Expanding characteristics of graphite in microwaveassisted exfoliation. Scientific Cooperations International Workshops on Engineering Branches, 273-277.
[9] Zhu Y, Murali S, Stoller MD, Velamakanni A, Piner RD, Ruoff RS. (2010). Microwave assisted exfoliation and reduction of graphite oxide for ultracapacitors. Carbon, 48:2118-2122.
[10] Sykam N, Kar KK. (2014). Rapid synthesis of exfoliated graphite by microwave irradiation and oil sorption studies. Materials Letters, 117:150-152.
[11] Toyoda M, Inagaki M. (2000). Heavy oil sorption using exfoliated graphite New application of exfoliated graphite to protect heavy oil pollution. Carbon, 38:199-210.
[12] Inagaki M, Toyoda M, Iwashita N, Nishi Y and Konno H. (2001). Exfoliated Graphite for Spilled Heavy Oil Recovery. Carbon Science, 2:1-8.
[13] Tryba B, Morawski AW, Kaleńczuk RJ, Inagaki M. (2003). Exfoliated Graphite as a New Sorbent for Removal of Engine Oils from Wastewater. Spill Science & Technology Bulletin 8:569-571.
[14] Zheng Y-P, Wang H-N, Kang F-Y, Wang L-N, Inagaki M. (2004). Sorption capacity of exfoliated graphite for oils-sorption in and among worm-like particles. Carbon, 42:2603-2607.
[15] Tryba B, Przepiórski J, Morawski AW. (2003). Influence of chemically prepared H_2SO_4-graphite intercalation compound (GIC) precursor on parameters of exfoliated graphite (EG) for oil sorption from water. Carbon, 41:2013-2016.
[16] Chung DDL. (2016). A review of exfoliated graphite. Journal of Materials Science 51:554-568.

[17] Cai M, Thorpe D, Adamson DH, Schniepp HC. (2012). Methods of graphite exfoliation. Journal of Materials Chemistry, 22:24992-25002,
[18] Ding X, Wang R, Zhang X, Zhang Y, Deng S, Shen F, Zhang X, Xiao H, Wang L. (2014). A new magnetic expanded graphite for removal of oil leakage. Marine pollution bulletin, 81:1885-1890.
[19] Wang G, Sun Q, Zhang Y, Fan J, Ma L. (2010). Sorption and regeneration of magnetic exfoliated graphite as a new sorbent for oil pollution. Desalination, 263:183-188.
[20] Lutfullin MA, Shornikova ON, Vasiliev AV, Pokholok KV, Osadchaya VA, Saidaminov MI, Sorokina NE, Avdeev VV. (2014). Petroleum products and water sorption by expanded graphite enhanced with magnetic iron phases. Carbon, 66:417-425.
[21] Jin C, Dong JH, Li DX, Zhu MC, Zhang YC. 2011. Characterization and Application of Expanded Graphite Coated by Fe_3O_4 Nanoparticles. Advanced Materials Research, 356-360:554-557.
[22] Mallampati R, Xuanjun L, Adin A, Valiyaveettil S. (2015). Fruit Peels as Efficient Renewable Adsorbents for Removal of Dissolved Heavy Metals and Dyes from Water. ACS Sustainable Chemistry & Engineering, 3:1117-1124.
[23] Huang Y, Li S, Chen J, Zhang X, Chen Y. (2014). Adsorption of Pb(II) on mesoporous activated carbons fabricated from water hyacinth using H_3PO_4 activation: Adsorption capacity, kinetic and isotherm studies. Applied Surface Science, 293:160-168.
[24] Raad MT, Behnejad H, Jamal ME. (2016). Equilibrium and kinetic studies for the adsorption of benzene and toluene by graphene nanosheets: a comparison with carbon nanotubes. Surface and Interface Analysis, 48:117-125.
[25] Yusuf M, Elfghi FM, Zaidi SA, Abdullah EC, Khan MA. (2015). Applications of graphene and its derivatives as an adsorbent for heavy metal and dye removal: a systematic and comprehensive overview. RSC Advances, 5:50392-50420.
[26] Yang X, Cui X. (2013). Adsorption characteristics of Pb (II) on alkali treated tea residue. Water Resources and Industry, 3:1-10.
[27] Pandey R, Ansari NG, Prasad RL, Murthy RC. (2014). Pb(II) Removal from Aqueous Solution by Cucumissativus (Cucumber) Peel: Kinetic, Equilibrium & Thermodynamic Study. American Journal of Environmental Protection, 2:51-58.
[28] Fan M, Li T, Hu J, Cao R, Wu Q, Wei X, Li L, Shi X, Ruan W. (2016). Synthesis and Characterization of Reduced Graphene Oxide-Supported Nanoscale Zero-Valent Iron (nZVI/rGO) Composites Used for Pb(II) Removal. Materials, 9:687-708.
[29] Gandha K, Elkins K, Poudyal N, Ping Liu J. (2015) Synthesis and characterization of $CoFe_2O_4$ nanoparticles with high coercivity. Journal of Applied Physics, 117:1-4.
[30] Shi M, Zuo R, Xu Y, Jiang Y, Yu G, Su H, Zhong J. (2012). Preparation and characterization of $CoFe_2O_4$ powders and films via the sol–gel method. Journal of Alloys and Compounds, 512:1665-1670.
[31] Zhou C, Zhu H, Wang Q, Wang J, Cheng J, Guo Y, Zhou X, Bai R. (2017). Adsorption of mercury(II) with an Fe_3O_4 magnetic polypyrrole–graphene oxide nanocomposite. RSC Advances, 7:18466-18479.